

# Single nanohole and photonic crystal: wavelength selective enhanced transmission of light

P. N. Melentiev,<sup>1</sup> A. E. Afanasiev,<sup>1</sup> A. A. Kuzin,<sup>2</sup> A. V. Zablotskiy,<sup>2</sup> A. S. Baturin,<sup>2</sup>  
and V. I. Balykin<sup>1,\*</sup>

<sup>1</sup>*Institute for Spectroscopy Russian Academy of Sciences, Phizicheskaya str., 5, Troitsk, Moscow reg., 142190, Russia*

<sup>2</sup>*Moscow Institute of Physics and Technology, Institutskiy per., 9, Dolgoprudniy, Moscow reg., 141700, Russia*  
[balykin@isan.troitsk.ru](mailto:balykin@isan.troitsk.ru)

**Abstract:** For the first time we have demonstrated an approach to control transmission of light through a single nanohole with the use of photon crystal microcavity. By use of the approach 28-fold enhanced transmission of light through a single nanohole in Au film has been experimentally demonstrated. The approach has the following advantages: (1) it enables to considerably increase transmission of light through *a single nanohole*, (2) the increase in transmission is unaffected by the hole diameter, (3) the transmission of nanohole is selective in frequency, the width of the resonance  $\sim \lambda/90$ , (4) no auxiliary structures are necessary on the surface of the Au film (extra nanoholes, grooves, etc.).

©2011 Optical Society of America

**OCIS codes:** (310.6628) Subwavelength structures, nanostructures; (050.1220) Apertures; (350.4238) Nanophotonics and photonic crystals; (310.4165) Multilayer design; (260.2710) Inhomogeneous optical media.

---

## References and links

1. C. Wieman, D. Pritchard, and D. Wineland, "Atom cooling, trapping, and quantum manipulation," *Rev. Mod. Phys.* **71**(2), S253–S262 (1999).
2. V. I. Balykin, "Atom optics and nanotechnology," *Phys. Usp.* **52**(3), 1 (2009).
3. T. W. Ebbesen, H. J. Lezec, H. F. Ghaemi, T. Thio, and P. A. Wolff, "Extraordinary optical transmission through sub-wavelength hole arrays," *Nature* **391**(6668), 667–669 (1998).
4. F. J. Garcia-Vidal, L. Martín-Moreno, T. W. Ebbesen, and L. Kuipers, "Light passing through subwavelength apertures," *Rev. Mod. Phys.* **82**(1), 729–787 (2010).
5. E. Moreno, A. I. Fernández-Domínguez, J. I. Cirac, F. J. García-Vidal, and L. Martín-Moreno, "Resonant transmission of cold atoms through subwavelength apertures," *Phys. Rev. Lett.* **95**(17), 170406 (2005).
6. H. A. Bethe, "Theory of diffraction by small holes," *Phys. Rev.* **66**(7-8), 163–182 (1944).
7. C. J. Bouwkamp, *Diffraction theory*, (London: Physical Society 1954).
8. F. J. García de Abajo, "Colloquium: light scattering by particle and hole arrays," *Rev. Mod. Phys.* **79**(4), 1267–1290 (2007).
9. A. Krishnan, T. Thio, T. J. Kim, H. J. Lezec, T. W. Ebbesen, P. A. Wolff, J. Pendry, L. Martín-Moreno, and F. J. García-Vidal, "Evanescence-coupled resonance in surface plasmon enhanced transmission," *Opt. Commun.* **200**(1-6), 1–7 (2001).
10. F. Kalkum, M. Peter, G. Barbastathis, and K. Buse, "External-resonance-enhanced transmission of light through sub-wavelength holes," *Appl. Phys. B* **100**(1), 169–172 (2010).
11. E. Popov and N. Bonod, "Physics of extraordinary transmission through subwavelength hole arrays," in *Structured surfaces as optical metamaterials*, A. A. Maradudin ed., (Cambridge: Cambridge University Press 2011), pp. 1–27.
12. E. Yablonovitch, "Inhibited spontaneous emission in solid-state physics and electronics," *Phys. Rev. Lett.* **58**(20), 2059–2062 (1987).
13. S. John, "Strong localization of photons in certain disordered dielectric superlattices," *Phys. Rev. Lett.* **58**(23), 2486–2489 (1987).
14. C. M. Kuznetsova and M. A. Okatova, *Handbook of Optics – Technologist* (Mashinostroenie Leningradskoe otdelenie 1983) (in russian).
15. M. Born and E. Wolf, *Principles of Optics* (Pergamon 1970).
16. P. N. Melentiev, A. V. Zablotskiy, D. A. Lapshin, E. P. Sheshin, A. S. Baturin, and V. I. Balykin, "Nanolithography based on an atom pinhole camera," *Nanotechnology* **20**(23), 235301 (2009).
17. D. P. Adams, M. J. Vasile, V. Hodges, and N. Patterson, "Focused ion beam fabrication of nanopores in metal and dielectric membranes," *Microsc. Microanal.* **13**(S02), 1512–1513 (2007).

18. D. R. Baer, M. H. Engelhard, A. S. Lea, P. Nachimuthu, T. C. Droubay, J. Kim, B. Lee, C. Mathews, R. L. Opila, L. V. Saraf, W. F. Stickle, R. M. Wallace, and B. S. Wright, "Comparison of the sputter rates of oxides films relative to the sputter rate of SiO<sub>2</sub>," *J. Vac. Sci. Technol. A* **28**(5), 1060–1072 (2010).
19. D. W. Pashley, M. J. Stowell, M. H. Jacobs, and T. J. Law, "The growth and structure of gold and silver deposits formed by evaporation inside an electron microscope," *Philos. Mag.* **10**(103), 127–158 (1964).
20. M. J. Lockyear, A. P. Hibbins, J. R. Sambles, and C. R. Lawrence, "Surface-topography-induced enhanced transmission and directivity of microwave radiation through a subwavelength circular metal aperture," *Appl. Phys. Lett.* **84**(12), 2040 (2004).
21. J. D. Jackson, *Classical Electrodynamics* (Wiley, 1962).
22. K. J. Koerkamp, S. Enoch, F. B. Segerink, N. F. van Hulst, and L. Kuipers, "Strong influence of hole shape on extraordinary transmission through periodic arrays of subwavelength holes," *Phys. Rev. Lett.* **92**(18), 183901 (2004).
23. P. N. Melentiev, A. E. Afanasiev, V. V. Klimov, V. I. Balykin, A. A. Kuzin, A. V. Zablotskiy, A. S. Baturin et al., preparing a manuscript to be called "Polarization sensitive transmission of a single nanohole embedded in a photonic crystal nanocavity".
24. V. I. Balykin, V. V. Klimov, and V. S. Letokhov, "Atom nanooptics," in *Handbook of Theoretical and Computational Nanotechnology*, M. Rieth M., W. Schommers eds., (Elsevier 2006), pp. 1–78.
25. E. Altewischer, M. P. van Exter, and J. P. Woerdman, "Plasmon-assisted transmission of entangled photons," *Nature* **418**(6895), 304–306 (2002).
26. J. Vučković, M. Loncar, and A. Scherer, "Surface plasmon enhanced light-emitting diode," *IEEE J. Quantum Electron.* **36**(10), 1131–1144 (2000).
27. A. Nahata, R. A. Linke, T. Ishi, and K. Ohashi, "Enhanced nonlinear optical conversion from a periodically nanostructured metal film," *Opt. Lett.* **28**(6), 423–425 (2003).
28. M. Notomi, "Manipulating light with strongly modulated photonic crystals," *Rep. Prog. Phys.* **73**(9), 096501 (2010).

## 1. Introduction

Propagation of waves (both electromagnetic and de Broglie matter waves) through holes in a screen has always been of a great fundamental and practical interest. The first experiments on transmission of light through holes formed the basis for the classical optics and have infinite number of practical applications. Propagation of material particles through holes has proved wave nature of material particles, and subsequently was crucial in development of atom optics [1] and atom lithography [2].

One of the important characteristics for particles propagation through a hole is the flux of transmitted particles. When holes diameter is smaller than the corresponding wavelengths, the diffraction impose restrictions on their use and, accordingly, limits possible applications. Therefore, the discovery of extraordinary optical transmission (EOT) phenomenon [3] has attracted considerable interest among scientists. The following fundamental research in the area has made the subwavelength hole as a new optical element [4]. Nowadays a new class of optical elements has been created around the EOT effect, including light emitting diodes, selective polarization filters, and energy concentrators. There is a suggestion to realize the extraordinary optical transmission with matter waves [5].

In the implementation of the EOT conditions, the ratio of the energy transmitted through the screen with a hole to the energy incident on the hole may exceed one and several orders of magnitude higher than the value predicted by the Bethe's diffraction theory for the subwavelength holes [6–8]. The increased transmission of radiation is based on multiple factors, the major of them are excitation of surface (plasmon) waves and proper arrangement of the holes in the screen, and for single holes – excitation of surface waves and periodic corrugations around apertures [4]. The transmission of subwavelength hole arrays can be enhanced further by a Fabry – Pérot type constructive interference [9, 10].

A shortcoming of the EOT in several applications is defined by the mechanism of its occurrence: excitation of plasmon waves and Fabry–Pérot resonances, resulting, in its turn, in effective use of the EOT only for: (1) relatively large holes, having a diameter just below the cut-off of the fundamental mode of a hole [11]; (2) holes in a screen made of highly-conductive materials (mainly, gold and silver); (3) periodical structures; and (4) limited number of applications, as the frequency resonances of the transmitted radiation are wide.

In this paper, another approach to realize the EOT is considered. It is based on placing a nanohole into radiation field of a 1D photonic crystal. Photonic crystals were proposed over

two decades ago to realize strong light confinement via their perfect photonic bandgaps [12, 13].

Among great variety of micro- and nanocavities the photonic crystals are one of the most promising objects for studying quantum-electrodynamics effects, because their Q-factor may be as high as  $10^6$ . Quantum-mechanical system placed into a photonic crystal manifests physical properties different from those of the system in a free space, in particular, enhancement of spontaneous emission near the photonic band edges, second-harmonic generation, and others [12]. Propagation of light through a nanohole can be simulated to a good accuracy with the use of the Babine principle, which allows one to replace the nanohole by a nanodisc, characterized by the corresponding (magnetic and electric) dipole moments, as was originally done by Bethe in his work [6]. As is well known, radiation of a dipole placed into a resonator is different from those in a free space. The main idea of this paper is to realize conditions, at which nanohole (effective dipole) is placed into region with maximum electromagnetic field of light in a 1D photonic crystal. The realized conditions can increase the emission rate of the effective dipole, and let to increase the total power of light emitted into free-space radiative modes on the exit side of the nanohole.

## 2. Photonic crystal microcavity

### 2.1 Photonic crystal microcavity without nanohole

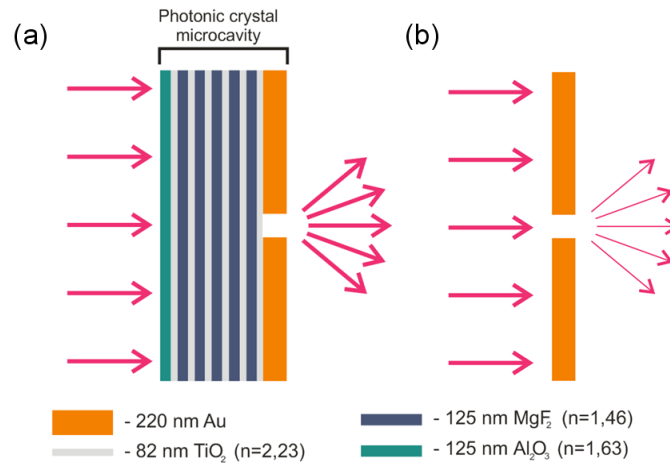


Fig. 1. Schematic diagram of samples under study: (a) single nanohole with diameter of 60 nm in 220 nm thick Au film, comprising the last layer of photonic crystal microcavity, (b) single nanohole with diameter of 60 nm in 220 nm thick Au film.

The 1D photonic crystal microcavity (PCM) was fabricated on a quartz substrate. The PCM is formed by 12-layer stack of alternating high-index ( $\text{TiO}_2$ ,  $n = 2.23$ ) and low-index ( $\text{MgF}_2$ ,  $n = 1.38$ ) dielectric layers of thickness  $\lambda/4n$  ( $\lambda = 730$  nm), coated on one side with optically thick 220 nm Au layer, Fig. 1(a) (indexes of refraction were taken from [14]). The 12-layer stack of dielectric layers forms 1D type photonic crystal, realizing low, about 2%, transmission of light in spectral range of 650 to 800 nm (a bandgap of the photonic crystal). Coating of the 1D photonic crystal by the 220 nm thick Au film realizes a photonic crystal microcavity with Q-factor around 100.

Analytic transfer-matrix formalism was used to calculate propagation of plane wave field through the PCM. The transfer of field through each layer of PCM is represented by 2 by 2 matrix, and the response of entire microcavity is represented by a product of these individual matrices, forming the so called characteristic matrix [15]:

$$M = M_1 M_2 \cdots M_{12} M_{Au} = \begin{bmatrix} m_{11} & m_{12} \\ m_{21} & m_{22} \end{bmatrix}, \quad (1)$$

$$M_j = \begin{bmatrix} \cos(kh_j) & i \sin(kh_j) / Y_j \\ i Y_j \sin(kh_j) & \cos(kh_j) \end{bmatrix}. \quad (2)$$

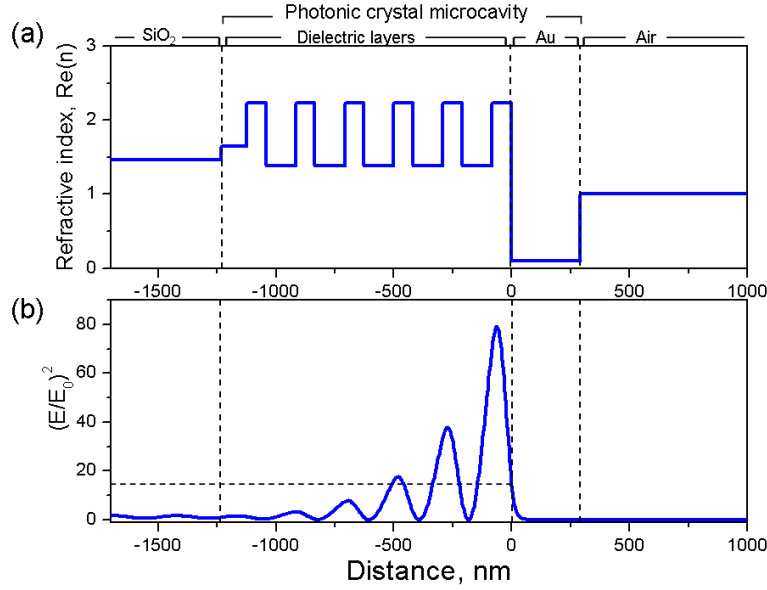


Fig. 2. Optical properties of the photonic crystal microcavity, being investigated in the paper: (a) microcavity refractive index stack design, (b) calculated resulting electric-field distribution for the PCM at resonant frequency  $\lambda = 789.6$  nm).

The characteristic matrix  $M$  relates the electric and magnetic fields ( $E$ ,  $H$ ) of the input and output of the photonic crystal microcavity:

$$\begin{bmatrix} E_{in} \\ H_{in} \end{bmatrix} = [M] \begin{bmatrix} E_{out} \\ H_{out} \end{bmatrix}, \quad (3)$$

$k = 2\pi / \lambda$  is a free-space wave vector of the incident light,  $h_j = n_j x$  (layer thickness) (Fig. 2(a)) with  $n_j$  the refractive index, and  $Y_j = [(\epsilon_0 / \mu_0)]^{1/2} n_j$ . Respectively, amplitude reflectance  $r$  and amplitude transmittance  $t$  are described by the expressions:

$$r = \frac{Y_0 m_{11} + Y_0 Y_s m_{12} - m_{21} - Y_s m_{22}}{Y_0 m_{11} + Y_0 Y_s m_{12} + m_{21} + Y_s m_{22}}, \quad (4)$$

$$t = \frac{2Y_0}{Y_0 m_{11} + Y_0 Y_s m_{12} + m_{21} + Y_s m_{22}}. \quad (5)$$

Figure 2(b) shows electric field  $E^2(r)$  distribution on the PCM axis at the microcavity's resonant frequency  $\lambda_{PCM} = 789.6$  nm, normalized to the square of the field amplitude of an incident plane wave  $E_0^2$  and calculated with the use of characteristic matrix approach. As illustrated, the field peaks up to  $E_{max}^2 \approx 80E_0^2$  in the TiO<sub>2</sub> layer adjacent to the Au film, and at

the  $\text{TiO}_2/\text{Au}$  boundary comes out to  $\approx 14E_0^2$ . Estimated cavity effective mode length is  $L_{\text{eff}} = \int \varepsilon(r) |E(r)|^2 dr / \varepsilon(r_{\text{max}}) |E(r_{\text{max}})|^2 \approx 0.17\lambda$ .

Figure 3(a) shows reflection spectrum of the PCM, as well as reflection spectrum of 1D photonic crystal calculated with the use of the characteristic matrix approach. Light impinging on samples was considered as a plane monochromatic polarized wave with a wave vector directed perpendicular to the plane of dielectric layers. The sharp resonance at  $\lambda_{\text{PCM}} = 789.6$  nm is a proof of microcavity formation, because without a microcavity there would be no minimum in reflection of a 1D photonic crystal. The resonance width is 6.6 nm, which corresponds to the quality factor of the microcavity:  $Q = \omega / \Delta\omega = 120$ . Despite the moderate value of the  $Q$ -factor, involved configuration of the PCM has an important feature: *light field is considerably enhanced nearby the Au film surface*.

We note some important features of the PCM's chosen configuration:  $\text{Al}_2\text{O}_3$  ( $n = 1.63$ ) layer between quartz substrate and  $\text{TiO}_2$  layer decreases the refractive index step in the direction of light field propagation and is necessary to increase the field amplitude of the microcavity's resonance mode. The chosen optical thickness of the Au film makes it possible to realize light reflectance at the  $\text{TiO}_2/\text{Au}$  boundary about 98%, which is necessary to form microcavity with  $Q \sim 100$ , as well as strongly decrease light transmission through the Au film.

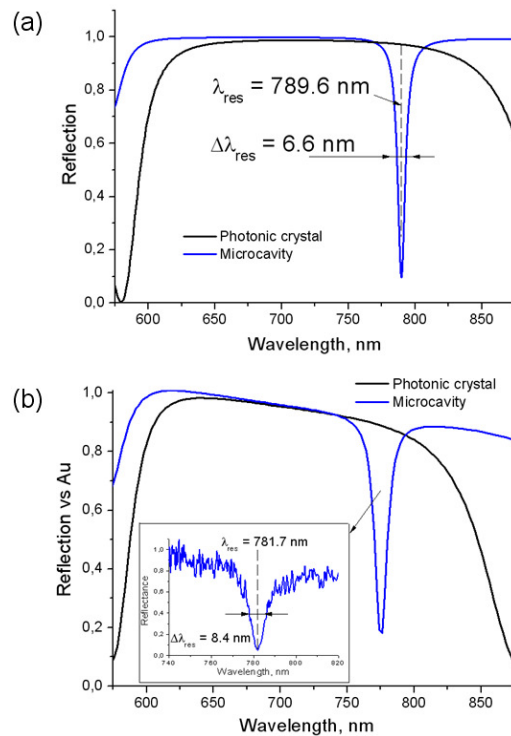


Fig. 3. Reflection spectra of the photonic crystal microcavity and forming it 1D photonic crystal: (a) calculated with use of characteristic matrix approach, (b) experimentally measured at  $12^\circ$  to the axis of the crystal (reflection spectrum at normal incidence angle is shown in the inset).

In the experimental implementation of photonic crystal microcavity the dielectric layers were deposited on the quartz substrate by the method of high-vacuum ion-assisted deposition, the Au film was deposited by thermal evaporation. PCM preparation was carried out under the conditions of Class 100 cleanroom. Thickness of Au film of the PCM equals to  $220 \pm 20$  nm and was measured by atomic force microscope with use of the razor blade scratch technique.

Measured roughness of the Au film surface is as follows: height roughness (RMS) equals to about 3 nm, lateral roughness (correlation length) equals to about 30 nm. Figure 3(b) shows reflection spectra, measured with spectrophotometer Specord-400, of both PCM and forming it 1D photonic crystal at  $12^\circ$  to the axis of the crystal. The figure shows that in the bandgap area of the photonic crystal coated with Au film a resonance is appeared, indicating formation of a cavity. Spectrophotometer Specord-400 gives no way of measuring reflection spectra at angles less than  $12^\circ$  to the axis of the PCM, with a consequent considerable shift of the measured resonance line. The exact value of the resonance was determined in a separate experiment on illuminating the PCM perpendicularly to the plane of its layers by collimated radiation of a halogen lamp and detecting with a spectrometer of “MORS” company (the reflection spectrum is shown in the inset of Fig. 3(b)). The PCM’s resonance frequency corresponds to  $\lambda_{\text{res}} = 781.7$  nm, and the width  $\Delta\lambda_{\text{res}} \approx 8.4$  nm, which corresponds to the  $Q$ -factor of 93.

Measuring of the microcavity’s mode characteristics, like intensity and effective length, is a complex physical problem. But for the investigated configuration of the MPC it is possible to determine the field intensity of the wave incident on the boundary  $\text{TiO}_2/\text{Au}$  inside the microcavity using measured data of the reflection spectrum. According to the energy conservation law:

$$I_0 = R_{\text{PCM}}^{\text{res}} I_0 + (1 - R_{\text{TiO}_2/\text{Au}}) I_{\text{TiO}_2}, \quad (6)$$

where  $I_0$  – intensity of the incident wave,  $R_{\text{PCM}}^{\text{res}} \approx 0.046$  – measured reflectance of the PCM at resonance,  $(1 - R_{\text{TiO}_2/\text{Au}}) I_{\text{TiO}_2}$  – intensity of the light absorbed in the Au layer,  $R_{\text{TiO}_2/\text{Au}} \approx 0.971$  – calculated value of the boundary  $\text{TiO}_2/\text{Au}$  reflectance. From Eq. (6) follows  $I_{\text{TiO}_2} = (1 - R_{\text{PCM}}^{\text{res}}) / (1 - R_{\text{TiO}_2/\text{Au}}) I_0 \approx 33 I_0$ , and maximum of the squared resonance mode amplitude is about of  $86 E_0^2$ . Measured characteristics of the microcavity’s mode have a good correlation with calculated ones. Discrepancies are accounted for by neglect in calculation of existing losses in dielectric layers, as well as finite accuracy of the PCM’s layers thickness control in the experiment.

## 2.2 Photonic crystal microcavity with nanohole

We used focused ion beam machine FEI Quanta 3D ( $\text{Ga}^+$  ions, 30 keV, focused on the Au film to a 10 nm diameter spot) to mill an array of circular apertures of about 60 nm diameter in an Au layer on a quartz substrate and in an Au layer of the PCM. Microscopy of nanoholes was conducted by electron microscope JEOL JSM-7001F with spatial resolution about 5 nm. To diminish intensity of carbon deposition process associated with electron beam microscopy of metallic surfaces, microscopy of nanoholes was carried out at relatively low electron beam energy of about 5 keV

Special attention was given to the problem of nanohole creation in the PCM. At simplified consideration, formation of a nanohole occurs through knocking out of a single Au atom by a single ion of the beam. Under long exposure of Au film to ion beam, not only forming of a nanohole take place but also the PCM’s dielectric layer adjacent to the Au film is destroyed. This results in deterioration of local characteristics of the microcavity’s mode nearby the nanohole. With too short exposure, an open-end hole is not formed in Au film, thus preventing a light field localized in microcavity from passing through the nanohole.

Optimal exposure time of the ion beam (ion doze) was determined in a separate experiment on making nanoholes in Au film deposited on an ultrathin free standing  $\text{SiO}_2$  film 40 nm thick [16]. Utilization of an ultrathin free standing film allowed (1) to control flux of ions transmitted through a nanohole [17], (2) to carry out microscopy of a hole from both sides of the film. Image contrast in electron microscopes is sensible to the material of the object under investigation, allowing to identify the  $\text{SiO}_2/\text{Au}$  boundary inside a nanohole and to determine the dimensions of  $\text{SiO}_2$  film destruction.

The Au film was created on the ultrathin free standing film simultaneously with gold deposited on 1D photonic crystal while manufacturing microcavity, thus ensuring equal Au film thickness in microcavity and on SiO<sub>2</sub> film. After a number of experiments the optimum ion dose of 4 pC at the 10 pA current of a focused ion beam has been chosen. Using these parameters of the ion beam a nanohole created in Au film has the following characteristics: on the SiO<sub>2</sub>/Au interface its diameter is around 60 nm, the walls of the opening are nearly – vertical (deviation from the vertical is about 5°). It is important that in the SiO<sub>2</sub> film the hole is not an open-end one on the SiO<sub>2</sub>/air interface. From this results the conclusion that the SiO<sub>2</sub> film destruction along the hole axis is less than 40 nm (a thickness of the SiO<sub>2</sub> film). Basing on the results of the work [18], we believe that while manufacturing a nanohole in a PCM with the chosen ion-beam dose the destruction depth of TiO<sub>2</sub> layer, adjacent to the Au film, is even smaller. In the work [18] it was shown that at identical parameters of an ion beam the etching rate for TiO<sub>2</sub> film is approximately 2 times lower than that for SiO<sub>2</sub> film. Basing on the data, our estimate for the destruction depth of TiO<sub>2</sub> layer nearby a PCM's nanohole is that it is no more than 20 nm.

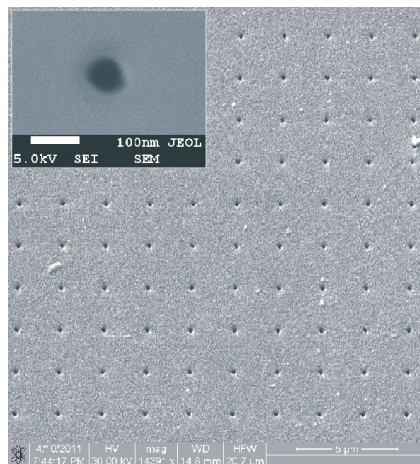


Fig. 4. Electron-microscope image of the nanoholes array made in Au layer of photonic crystal microcavity. Enlarged image of a one nanohole is shown in the inset.

We prepared two samples to investigate the PCM's influence on optical properties of nanoholes: (1) nanoholes in an Au layer of the PCM, (2) nanoholes in a reference Au film deposited on a 2 mm thick SiO<sub>2</sub> substrate. The thickness of the reference Au film was equal to that of the PCM's Au layer. By ion beam with above-defined parameters, matrices of 10×10 identical nanoholes were produced in each sample, the distance between the nanoholes being 2 μm (Fig. 4). Electron-microscope image of one of the matrices' nanohole is shown in the inset of Fig. 4. An analysis of the images has shown that there is dispersion of nanoholes' dimensions and geometries: (a) about 60% of the holes have round shape with diameter 58 (± 5) nm, (b) some holes have ellipticity with maximum dispersion of the ellipse axis 2a = 54 nm, 2b = 63 nm. The dispersion of nanoholes' dimensions and geometries is associated with surface inhomogeneity of the Au film produced by the method of thermal evaporation to the surface of dielectric, what by virtue of Au atoms' high surface energy results in the formation of nanocrystals in the Au film [19].

### 3. Light transmission by single nanohole embedded in photonic crystal microcavity

Figure 5 shows a schematic of the nanohole embedded in 1D photonic crystal microcavity and the setup for microscopic imaging and transmission spectroscopy. The samples with nanoholes (Fig. 1) were illuminated at normal incidence with a halogen lamp light collimated to ± 3°. Halogen lamp light was passing through fiber to ensure homogeneous illumination of the sample. To study the role of possible collective effects for light transmission by single

nanohole, measurements were also taken, when the illuminated light was filtered by use of a single mode fiber and focused by 10x (NA=0.3) objective to a spot with diameter of about 2  $\mu\text{m}$  (FWHM) in the plane of the nanohole, realizing illumination of single nanohole. Special design of samples was implemented to control the values of the intensity of illuminating light: part of the substrate's surface in both samples was free from optical coatings. Transmitted light was collected with a 100x Nikon microscope objective (NA=1.49), and analyzed through: (1) a band pass filter using a 2D cooled CCD camera with avalanche gain (Princeton Instruments), or (2) a monochromator with a high optical efficiency, coupled to another cooled CCD camera (Princeton Instruments). For both samples index-matching fluid was applied to the Au-air interface to realize maximum collection efficiency of the objective lens.

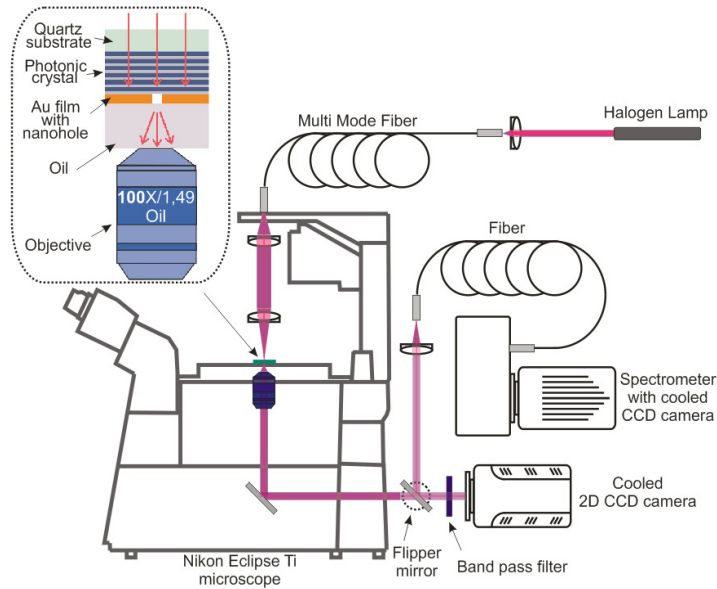


Fig. 5. Experimental setup for measurement the transmission of a single nanohole.

The experimental setup was allowed to obtain 2D optical image of single nanohole with spatial resolution of about 300 nm. The transmission spectrum of single hole was determined by two methods: (1) measuring transmission spectrum of a nanoholes matrix by a spectrometer with following normalization to the number of nanoholes, the method made it possible to obtain spectra with resolution around 0.7 nm; (2) measuring signal of a single nanohole image on a 2D CCD at various transmission wavelengths of band pass filters mounted before the 2D CCD, making it possible to obtain transmission spectra with resolution around 10 nm.

In the analysis of the transmission spectra of a nanohole, we define the parameter  $Q_{Em}(\lambda)$  as the total power emitted into free-space radiative modes on the exit side of the nanohole,  $g$  – collection efficiency of the objective,  $I(\lambda)$  – incident light intensity,  $S$  – nanohole area. Nanohole transmission was defined as  $T(\lambda) = Q_{Em}(\lambda)/(g \times I(\lambda) \times S)$ . Angle of light collection for the objective with NA=1.49 equals to about  $160^\circ$ . Measurement of angular dependence of light emitted by subwavelength aperture is a separate complicated problem [20]. For the sake of simplicity we assumed that  $g = 1$ , by approximately 20% underestimating the measured values for transmission in the case of a hole in an infinitely thin screen, when emitted light of a single nanohole is diffracted nearly isotropically. In our configuration the length of the channel formed by a hole in the Au film is 3.6 times larger than the hole's diameter, and the light emerging from a nanohole propagates in space nonisotropically: calculations show that the radiation is concentrated mainly in a  $150^\circ$  cone [21]. In this case  $g = 1$  is a good approximation as more than 95% of the photons leaving the hole are collected by the objective.



To avoid errors associated with differences in spectral sensitivity of various photodetectors and in spectral transmission of various optical instruments,  $I(\lambda)$  and  $Q_{Em}(\lambda)$  were measured in the microscope with the use of the same objective and the same CCD camera. Let us note that flux density of the photons that were passing through the nanohole is several orders greater than that of the photons that were passing through the Au film. This allowed in the experiment to detect photons passing through the nanohole on a practically zero background.

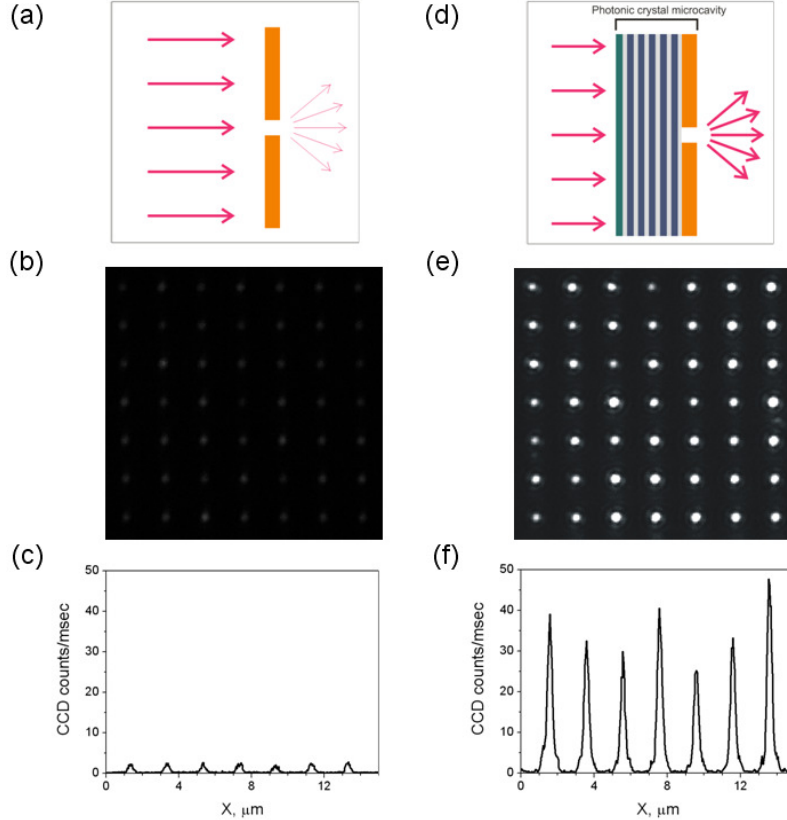


Fig. 6. Transmissions of nanoholes in the Au film and nanoholes in the photonic crystal microcavity at identical parameters of illumination and detection at a light wavelength nearby the PCM's resonance mode: *Left column* – nanoholes in the Au film: (a) the scheme of nanoholes illumination in the reference Au film, (b) nanoholes images of the reference Au film in the 2D CCD of the microscope, (c) cross-section of the images for the nanoholes in the reference Au film. *Right column* – nanoholes in the photonic crystal microcavity: (d) the scheme of nanoholes illumination in the photonic crystal microcavity, (e) nanoholes images of the photonic crystal microcavity in the 2D CCD of the microscope, (f) cross-section of the images for the nanoholes produced in the PCM.

Figure 6 shows images of nanoholes in the reference Au film and nanoholes in the Au film of the PCM at a light wavelength nearby the PCM's resonance mode, obtained with the experimental setup depicted in Fig. 5 and the use of a band pass filter with central wavelength of transmission  $\lambda_{\text{filter}} = 780$  nm and width  $\Delta\lambda_{\text{filter}} = 10$  nm mounted before the 2D CCD. The images were obtained at identical parameters of samples illumination and detection. 2D images of nanoholes (Fig. 6(b), 6(e)) indicate that the image signal amplitude for nanoholes in the reference Au film is so small that they are practically invisible, while the image signal amplitude for nanoholes in the microcavity is so high that it exceeds the dynamic range of signal representation in 2D. This means that at identical parameters of incident radiation the flux of photons emitted into free-space radiative modes on the exit side of nanoholes produced in the PCM is significantly higher than that for nanoholes in the reference Au film. The fact is

a direct proof of influence of the photonic crystal microcavity on the nanoholes transmission enhance.

Figure 6 shows that the image signal amplitude for nanoholes produced both in the PCM and in the reference Au film (Fig. 6(b)) varies from hole to hole. For some holes the difference is as much as about 100%. So dramatic variation in the transmitted light intensity is impossible to be accounted for only by the well-known dependence of nanoholes transmissibility on their form, diameter, and geometry [22]. Our separate publication [23] will describe strong dependence of transmission of a nanohole embedded in PCM on nanohole's geometry and polarization of incident radiation.

With the help of nanoholes' electron-microscope images we established a one-to-one correspondence between the power of radiation transmitted through each individual nanohole (Fig. 6) and their exact dimensions and geometry. It turned out that for round holes 60 nm in diameter the signal amplitude through a nanohole in the reference Au film is 3.5 counts/ms, while for nanoholes in the PCM it is 65 counts/ms. A consideration of band pass filter's central band displacement from the PCM's resonance gives correction factor of 1.53. Hence the measured photons flux enhance at the resonance wavelength of the microcavity emitted on the exit side of the nanoholes produced in the PCM approximately 28 times exceeds that for nanoholes in the reference Au film.

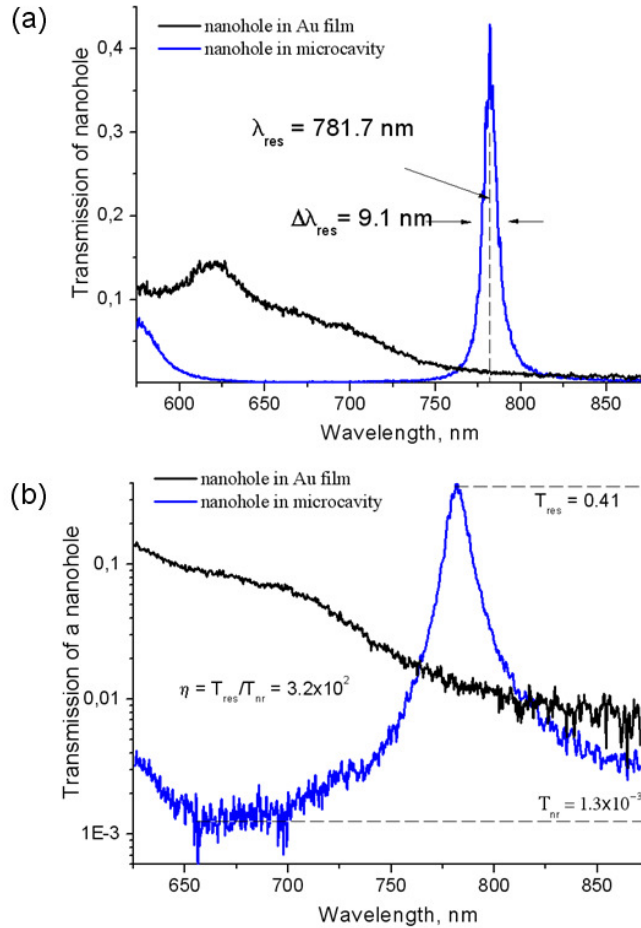


Fig. 7. Transmission spectra for a single nanohole in the reference Au film and for a single nanohole in the photonic crystal microcavity: (a) linear scale, (b) logarithmic scale.

In a separate experiment we investigated the effect of collective influence of nanoholes on their transmission. For this purpose, two regimes of nanoholes illumination by radiation (at the light wavelength of the resonance mode of microcavity) were utilized: (1) illumination of all  $10 \times 10$  nanoholes on the PCM and of the reference Au film; and (2) illumination of a single nanohole by a sharp focused radiation. In both cases a transmission signal of a single nanohole was registered with 2D CCD. Measured transmission for a single round nanohole of diameter 60 nm in the reference Au film was  $T_{\text{Au film}} \approx 1,5\%$  and for a corresponding nanohole in the PCM –  $T_{\text{PCM}} \approx 41\%$ . Measured values did not depend on a chosen scheme of nanohole illumination. Hence we have not found effects of collective influence of nanoholes on their transmission and total transmission of an array of nanoholes is therefore equal to the sum of transmissions through isolated holes.

Essential distinction in the nature of light transmission by a nanohole produced on PCM compared to a nanohole in a simple Au film is sharp frequency-selectivity. Figure 7(a) shows transmission spectra of nanoholes in a matrix measured with a spectrometer and then attributed to a single nanohole. The figure distinctly depicts the transmission resonance of nanohole in the PCM at the wavelength of the microcavity's resonance mode. The resonance width is roughly 9 nm corresponding to the spectral width of the microcavity's resonance mode. At wavelengths outside the microcavity's resonance the transmission of nanohole in the PCM is governed by the transmission of the 12-layer stack of the PCM (band gap of the 1D photonic crystal) and is considerably lower than the transmission of nanoholes in the reference Au film. In Fig. 7(b) the same spectra of a nanohole transmission are represented in the logarithmic scale. The minimum value of the transmission of nanohole in the PCM is about  $1.1 \times 10^{-3}$  and is realized at the light wavelength of 675 nm, being almost 300 times less than the transmission of PCM's nanohole in the resonance. Hence utilization of the microcavity makes it possible to realize high spectral selectivity of a single nanohole transmission.

#### 4. Discussion

The demonstrated experiments show that utilization of the photonic crystal microcavity allows one considerably enhances the photon flux at the exit of the nanohole. As a first approximation, the physics of the process reduces to the increase of light field at the location of PCM's nanohole. At the same time nanoholes also influence the properties of the microcavity, and a correct consideration assume that a PCM and a nanohole should be studied as a common physical system.

Diameters of the nanoholes chosen for this work are rather small and, as the measurements have shown, do not appreciably affect microcavity's properties, as follows from comparison of transmission spectra for nanoholes in the PCM (Fig. 7(a)) with the reflection spectrum of the nanoholeless microcavity (Fig. 3(b)). Quantitative measurements of nanohole transmission also confirm preservation of microcavity's resonance mode properties after production of nanoholes: 30-fold enhance of photons flux emitted at the exit of a nanohole agrees with approximately 30-fold enhanced intensity of the light wave illuminating the entrance of a nanohole into PCM as compared with the reference Au film.

The localized and propagating surface plasmon (SP) waves can strongly modify transmission of nanoholes made in metallic film, leading to enhancement or suppression of light transmission. In this paper we didn't study the role of SP on the light transmission. The transmission of nanoholes in Au film of the PCM was compared with the transmission of nanoholes in Au film on a quartz substrate. This allowed us to explore the sole influence of the PCM on transmission of nanoholes fabricated in Au film, without study the role of surface waves: the SP are excited both in the reference Au film and in the Au film of the PCM. A separate research is needed to account effect of SP waves. The two main facts demonstrate that the measured enhancement of transmission of a nanohole is attributed to the influence of the PCM cavity mode: (1) absence of SP like structure in measured transmission spectrum of nanohole in the reference Au film for wavelength of light around the PCM resonance (Fig. 7(a)), and (2) the sharp frequency resonance in transmission of nanohole in the PCM, with a width much smaller then the width of SP resonances in transmission spectrum for the array of

nanoholes. The excitation of SP in Au film of the PCM can further enhance transmission of nanoholes.

The measurements of a single nanohole transmission in PCM have shown that quantitative characteristics of a nanohole transmission (power, orientation, polarization characteristics, etc.) strongly depend on nanohole's dimensions and geometry [23], and therefore the determination of a single nanohole's optical properties should be combined with electron microscopy of the hole.

Illuminated by laser radiation, a single nanohole in a conductive screen is an example of light nanofield realization and has a number of important applications [24]. Microcavity may be used for enhanced light transmission through the nanoholes thus opening the way to multifold by intensity and selective by wavelength signal enhance for a number of applications, such as optical microscopy with nanoresolution, nanolithography utilizing light nanofields [24], quantum information science [25], sensing, data storage and light extraction from LED [26]. Moreover, in our sample second harmonic generation can be demonstrated with an enhanced efficiency: for a given input power, the intensity in the second harmonic can be increased by a factor of 900, since the second harmonic intensity follows the square of the excitation intensity.

By now the largest transmission enhancement reported is  $G = 125$  for a single hole with a set of concentric ring grooves, periodically spaced in the radial direction [27] and it is  $\sim 4$  times higher compared to our sample. In the experiment the localization of light field is determined by the diameter of concentric rings encircling the nanohole and ensuring the localization only in submicron range of dimensions. For our sample the spatial localization of light field is determined by the diameter of nanohole used and at its exit is equal to roughly 60 nm, making it possible to form a 2D nanofield with a record-high density of light field localized in nanoscale.

Another interesting perspective of application a photonic crystal microcavity to control transmission of apertures is to use of slits made in metal film of the PCM since for one particular polarization of incident light it can propagate inside slits whatever width of the slits (not cut-off condition): the slits with extremely small thickness can be used, realizing high intensity source of light localized in nm scale (in 1D).

In conclusion let us note the potentialities of the system «nanohole + photonic crystal microcavity». While in this work a microcavity with a fairly moderate Q-factor of  $\sim 100$  was used, the utilization of high-Q cavities with Q-factor of  $\sim 10^6$  [28] is a promising prospects for further investigations in the area.

### **Acknowledgments**

This work has been performed with partial support of the grants RFBR N° 11-02-00804-a and 09-02-01022-a, the Program of the Russian Academy of Sciences' Presidium «Extreme light fields». The equipment of CKP MIPT and REC "Nanotechnology" of MIPT has been used in this work.